Title

Verticillium dahliae Effector VdCE11 Contributes to Virulence by Promoting Accumulation and Activity of the Aspartic Protease GhAP1 from Cotton

Journal

Microbiology Spectrum, 11(1)

ISSN

2165-0497

Authors

Li, Chi
Qin, Jun
Huang, Yingqi
et al.

Publication Date

2023-02-14

DOI

10.1128/spectrum.03547-22

Peer reviewed

AMERICAN SOCIETY FOR MICROBIOLOGY | Microbiology Spectrum

RESEARCH ARTICLE

Verticillium dahliae Effector VdCE11 Contributes to Virulence by Promoting Accumulation and Activity of the Aspartic Protease GhAP1 from Cotton

Chi Li,[a] Jun Qin,[a] Yingqi Huang,[a] Wenjing Shang,[a] Jieyin Chen,[b,c] Steven J. Klosterman,[d] Krishna V. Subbarao,[e] Xiaoping Hu[a]

[a]State Key Laboratory of Crop Stress Biology for Arid Areas and College of Plant Protection, Northwest A&F University, Yangling, China
[b]State Key Laboratory for Biology of Plant Diseases and Insect Pests, Institute of Plant Protection, Chinese Academy of Agricultural Sciences, Beijing, China
[c]Western Agricultural Research Center, Chinese Academy of Agricultural Sciences, Changji, China
[d]Agricultural Research Service, U.S. Department of Agriculture, Salinas, California, USA
[e]Department of Plant Pathology, University of California—Davis, c/o U.S. Agricultural Research Station, Salinas, California, USA

ABSTRACT *Verticillium dahliae* is a soilborne plant fungal pathogen that causes *Verticillium* wilt, a disease that reduces the yields of many economically important crops. Despite its worldwide distribution and harmful impacts, much remains unknown regarding how the numerous effectors of *V. dahliae* modulate plant immunity. Here, we identified the intracellular effector VdCE11 that induces cell death and defense responses in *Nicotiana benthamiana* to counter leaf pathogens such as *Sclerotinia sclerotiorum* and *Botrytis cinerea*. VdCE11 also contributes to the virulence of *V. dahliae* in cotton and *Arabidopsis*. Yeast two-hybrid library screening and immunoprecipitation revealed that VdCE11 interacts physically with the cotton aspartic protease GhAP1. GhAP1 and its *Arabidopsis* homolog AtAP1 are negative regulators of plant immunity, since disruption of either increased the resistance of cotton or *Arabidopsis* to *V. dahliae*. Further, VdCE11 plays a role in promoting the accumulation of the AP1 proteins and increasing its hydrolase activity. Taken together, these results indicate a novel mechanism regulating virulence whereby the secreted effector VdCE11 increases cotton susceptibility to *V. dahliae* by promoting the accumulation and activity of GhAP1.

IMPORTANCE *Verticclium dahliae* is a plant fungal pathogen that causes a destructive vascular disease on a large number of plant hosts, resulting in great threat to agricultural production. In this study, we identified a *V. dahliae* effector VdCE11 that induces cell death and defense responses in *Nicotiana benthamiana*. Meanwhile, VdCE11 contributes to the virulence of *V. dahliae* in cotton and *Arabidopsis*. Yeast two-hybrid library screening and immunoprecipitation revealed that VdCE11 interacts physically with the cotton aspartic protease GhAP1. GhAP1 and its *Arabidopsis* homolog AtAP1 are negative regulators of plant immunity since disruption of either increased the resistance of cotton or *Arabidopsis* to *V. dahliae*. Further research showed that VdCE11 plays a role in promoting the accumulation of the AP1 proteins and increasing its hydrolase activity. These results suggested that a novel mechanism regulating virulence whereby VdCE11 increases susceptibility to *V. dahliae* by promoting the accumulation and activity of GhAP1 in the host.

KEYWORDS *Verticillium dahliae*, effector, plant immunity, aspartic protease

Verticillium dahliae is a soilborne pathogen that penetrates plant roots and colonizes the xylem (1–3). This pathogen has a wide host range, including ornamental shrubs to forest trees and numerous crops, and causes massive economic losses each year (2). *V. dahliae* can survive in the form of microsclerotia in soil for over 14 years (4). When the microsclerotia of *V. dahliae* are stimulated by host root exudates, they germinate and develop hyphae (1, 5). Hyphae adhere closely to the root surface and further differentiate to form penetration pegs that penetrate the plant root, traverse the cortex, and eventually colonize the xylem (1, 5–9).

Editor Junhyun Jeon, Yeungnam University

Address correspondence to Xiaoping Hu, xphu@nwsuaf.edu.cn.
The authors declare no conflict of interest.

Received 4 September 2022
Accepted 4 January 2023
Published 19 January 2023

V. dahliae is a hemibiotrophic pathogen that initially colonizes plants as a biotroph and later switches to a necrotrophic lifestyle during later phases of infection (10–13), phases that have also been described as parasitic and saprophytic, respectively (1). Like most plant pathogens, *V. dahliae* must overcome plant immunity during the biotrophic stage to achieve successful colonization of the host (3, 12). Two types of immunogenic signals trigger plant immunity. Pathogen-associated molecular patterns (PAMPs; also known as microbe-associated molecular patterns [MAMPs]), such as bacterial flagellin and fungal chitin, are recognized by plant plasma membrane-bound receptors (known as pattern recognition receptors [PRRs]) to induce the first layer of innate immunity (known as PAMP-triggered immunity [PTI]) (14, 15). Another type of immunogenic signal involves effectors which directly suppress PTI or scavenge PAMP molecules from recognition to facilitate pathogen infection (12, 16–19). Effectors are often isolate or lineage-specific, such as the Ave1 protein of *V. dahliae* (20) and may be recognized by plant resistance (R) proteins that activate the second layer of immunity (effector-triggered immunity [ETI]) often accompanied by localized cell death (12). PTI and ETI are initiated from either the extracellular space or intracellularly in the cytoplasm through the interaction between pathogen molecules and plant receptors, an interaction that causes signal transduction to the plant nucleus to activate expression of defense genes, accumulation of reactive oxygen species (ROS), and callose deposition (21–23).

The mechanisms of *V. dahliae* effector-mediated modulation of host immunity are progressively being unraveled (3), though relatively few "bona fide" effectors have been identified and functionally characterized in *V. dahliae* among the catalog of 780 predicted secreted proteins in *V. dahliae* isolate VdLs.17 (24). The famous *V. dahliae* effector protein, Ave1, interacts with the tomato resistance gene product Ve1, a membrane-bound receptor-like protein that confers resistance to isolates of *V. dahliae* carrying *Ave1* (20). It is unknown whether Ave1 functions inside host cells during *V. dahliae* infection. Another *V. dahliae* effector, VdIcs1, is an isochorismate synthase that can suppress salicylic acid (SA) signaling during host colonization (25). VdSCP41 localizes in the host nucleus and suppresses plant immunity by disrupting the transcriptional activity of the master immune regulators CBP60g and SARD1 (26). VdCUT11 is an apoplastic effector that induces cell death and triggers defense responses in *N. benthamiana*, cotton, and tomato (27). Virulence effector VdXyn4 functions in the nuclei and chloroplasts of plant cells, depends on endocytosis mediated by immune receptors BAK1 and SOBIR1 to avoid or delay VdXyn4 entry into the salicylic and jasmonic acid-mediated defense pathways, and ultimately leads to cell necrosis in plants vein tissue (28). These studies demonstrated that the *V. dahliae* effectors have evolved to target host regulatory proteins and disrupt host defense signaling networks to promote fungal pathogenicity.

Studies of *V. dahliae* effectors have provided valuable tools to aid in *Verticillium* wilt research and its management (13). Further elucidation of the role of effectors in *V. dahliae*-plant interactions holds promise for development of additional tools. In this study, we identified the *Verticillium dahliae* candidate effector (VdCE11) and thus primarily aimed to functionally characterized its role in *V. dahliae*-plant interactions. We demonstrate that VdCE11 causes cell death and activates defense responses in *N. benthamiana* leaves and contributing to the virulence of *V. dahliae* in cotton by promoting the accumulation and enzymatic activity of the cotton protease GhAP1 (*Gossypium hirsutum* aspartic protease 1), a negative regulator of plant immunity.

RESULTS

Identification of a *V. dahliae* effector that induces plant cell death. We had previously sequenced the whole genome of *V. dahliae* XJ592 and identified predicted 793 secreted proteins (29). From these 793 proteins, 67 candidate effectors were predicted in this study by bioinformatics analyses, based on the general features of classical effectors (see Table S1 in the supplemental material). These candidate effectors were transiently expressed in *N. benthamiana* leaves to screen for those that induce cell death (see Fig. S1). The Bcl-2-associated X (BAX) and the green fluorescent protein (GFP) controls resulted in cell death or no cell death, respectively. The candidate

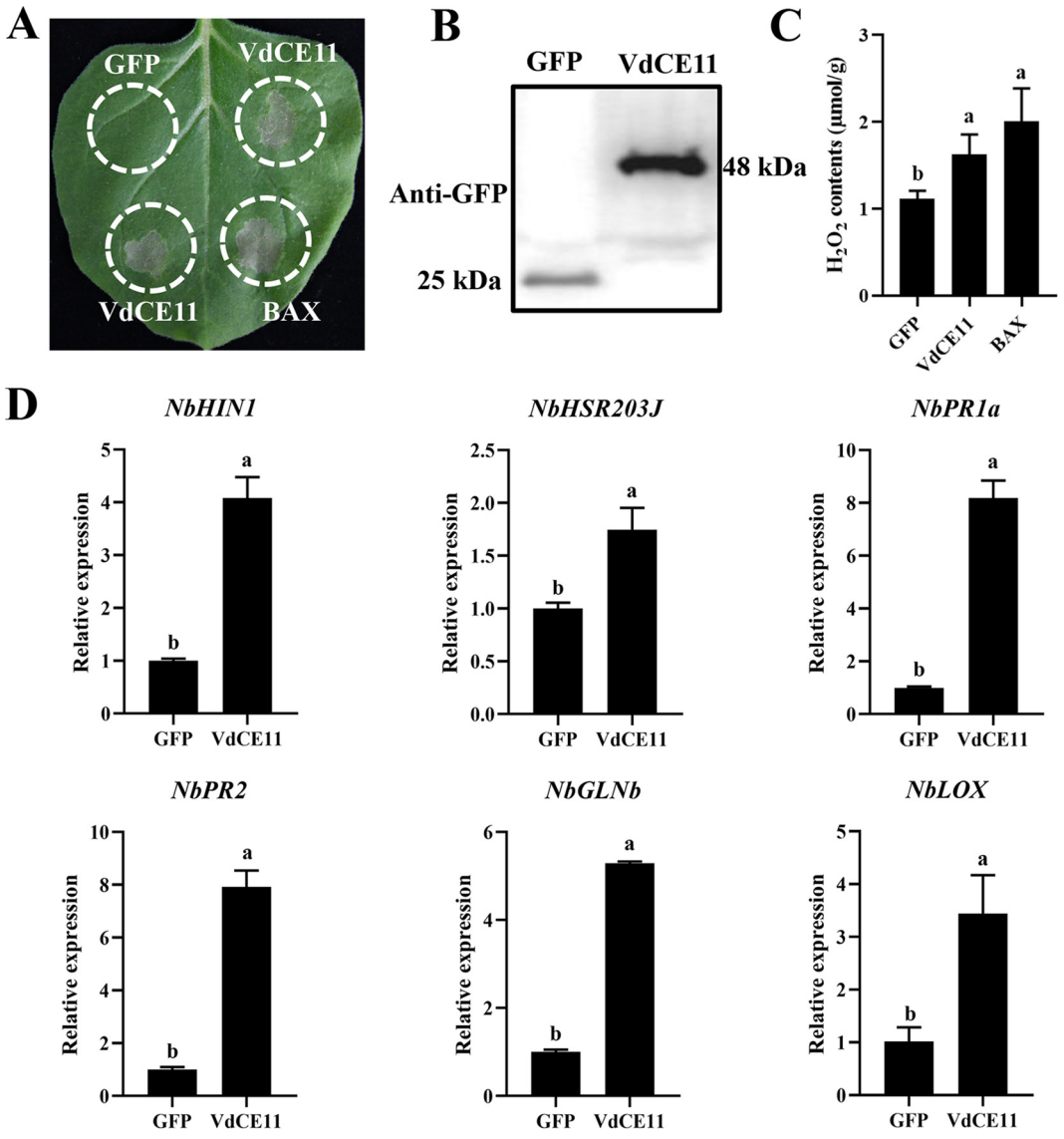

FIG 1 VdCE11 from *V. dahliae* induces plant immunity responses in *N. benthamiana*. (A) VdCE11 induces cell death in *N. benthamiana*. Four-week-old plants were infiltrated with *A. tumefaciens* carrying GFP, VdCE11-GFP, or BAX from pBin vectors for transient expression. Photographs were taken at 7 days after *Agrobacterium* infiltration. (B) Western blot (WB) analysis of transient expression of VdCE11 fused to the GFP tag in *N. benthamiana* leaves at 48 h after infiltration. (C) H_2O_2 contents of VdCE11 transiently expressed *N. benthamiana* leaves at 48 h after infiltration. (D) Relative expression of hypersensitive-response-specific and defense-related marker genes in *N. benthamiana* infiltrated with *A. tumefaciens* carrying the pBin-GFP, pBin-VdCE11-GFP, or pBin-BAX vectors. Total RNA was extracted at 48 h postinfiltration, and transcript levels were detected by RT-qPCR. The *NbEF-1α* gene was used as the internal reference gene for relative expression analyses. The data shown represent the means across three independent experiments. Different letters represent significant differences ($P < 0.05$), according to a Student *t* test. Bars indicate the standard error (SE).

effector VdCE11 induced cell death when expressed in *N. benthamiana* leaves (Fig. 1A and B). VdCE11 contains a predicted signal peptide (SP) at its *N terminus*. To assess the function of this SP in VdCE11, we conducted a secretion assay in yeast. The invertase mutant yeast strain YTK12 transformed with pSUC2-VdCE11SP construct could grow on the YPRAA medium, indicating the invertase is secreted (see Fig. S2A). The secretion of invertase was further confirmed using an enzymatic activity assay based on invertase-mediated conversion of the colorless dye 2,3,5-triphenyltetrazolium chloride (TTC) into the insoluble red colored triphenylformazan (TTF) (see Fig. S2B). These results demonstrated that the signal peptide of VdCE11 can mediate the secretor of VdCE11.

In addition to a signal peptide at the *N terminus*, VdCE11 also contains conserved

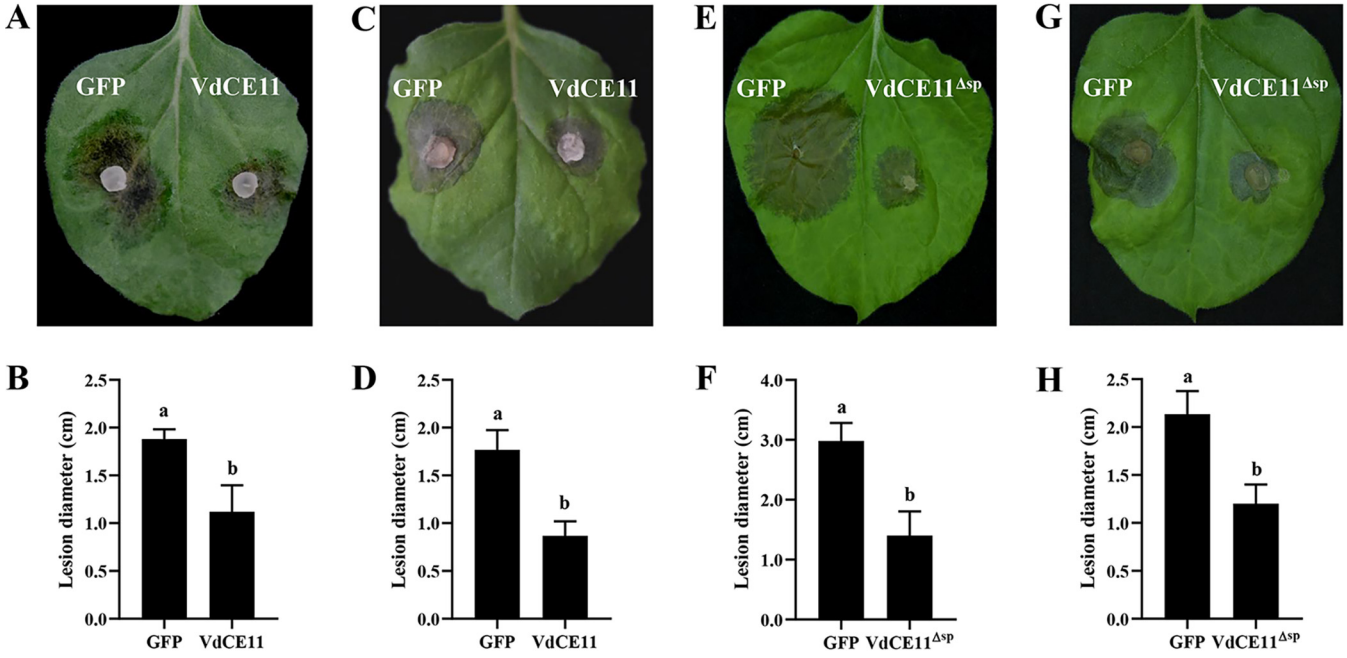

FIG 2 VdCE11 enhances the resistance of *N. benthamiana* to *S. sclerotiorum* and *B. cinerea*. *N. benthamiana* leaves were infiltrated with *A. tumefaciens* for transient expression of the indicated genes using pBin vectors. GFP was used as the negative control. (A) Symptoms of *N. benthamiana* leaves at 24 h postinoculation (hpi) with *S. sclerotiorum*. (B) Lesion diameter on *N. benthamiana* leaves following inoculation with *S. sclerotiorum*. (C) Symptoms of *N. benthamiana* leaves at 72 hpi with *Botrytis cinerea*. (D) Lesion diameter of *N. benthamiana* leaves after inoculation with *B. cinerea*. (E) Symptoms of *N. benthamiana* leaves at 24 hpi with *S. sclerotiorum*. (F) Lesion diameter of *S. sclerotiorum*-infected *N. benthamiana* leaves. (G) Symptoms of *N. benthamiana* leaves at 72 hpi. (H) Lesion diameter on *N. benthamiana* leaves following inoculation with *B. cinerea*. The data shown represent the means across three independent experiments. Different letters represent significant differences ($P < 0.05$), according to a Student *t* test. Bars indicate the SE.

homologs of *Cladopsorium fulvum* Ecp2 effector (Hce2) domain present in many fungi (see Fig. S3A and B) (19). BLAST analysis was performed on the *V. dahliae* XJ592 genome, revealing four Hce2 domain-containing proteins in *V. dahliae* XJ592 in addition to VdCE11 (see Fig. S3A and B and Table S2). To identify whether Hce2 domain-containing proteins contribute to a hypersensitive response (HR), each was expressed in *N. benthamiana*. None of the other proteins caused cell death when expressed in *N. benthamiana* (see Fig. S3C), suggesting that VdCE11 plays a important role in the regulation of the plant immune response.

VdCE11 triggers plant immunity responses. To determine whether VdCE11-activated cell death was associated with plant immune responses, we examined ROS accumulation, together with the expression of two HR-specific marker genes, *NbHIN1* and *NbHSR203* (30, 31), in *N. benthamiana*. The accumulation of H_2O_2 was significantly higher when VdCE11 was expressed than that in the GFP control (Fig. 1C). In addition, the expressions of *NbHIN1* and *NbHSR203J* were upregulated by VdCE11 expression (Fig. 1D). These results suggested that VdCE11 can activate HR-associated immune responses.

To clarify whether VdCE11-activated immunity was accompanied by alteration of hormone signaling pathways, the expression level of four defense-related marker genes were examined. These genes include (i) *NbPR1a*, *NbPR2*, and *NbGLNb*, marker genes of SA-dependent immunity pathway (32, 33), and (ii) *NbLOX*, marker gene of jasmonic acid (JA)-dependent immunity pathway (34). As shown in Fig. 1D, the expression levels of all four were significantly higher in VdCE11-expressed samples compared to the GFP control. These findings indicated that VdCE11 triggers immunity by activation of the SA- and JA-mediated defense pathways.

To study whether VdCE11 enhances plant resistance against phytopathogenic fungi, *Botrytis cinerea* and *Sclerotinia sclerotiorum* were inoculated onto areas of *N. benthamiana* leaves where VdCE11 and VdCE11$^{\Delta sp}$ was expressed and the diameters of the lesions were measured (Fig. 2A, C, E, and G). As shown in Fig. 2B, D, F, and H, the lesion diameters caused by *S. sclerotiorum* or *B. cinerea* were significantly decreased in both VdCE11- or VdCE11$^{\Delta sp}$-expressing leaves compared to the GFP control. These results strongly indicated that

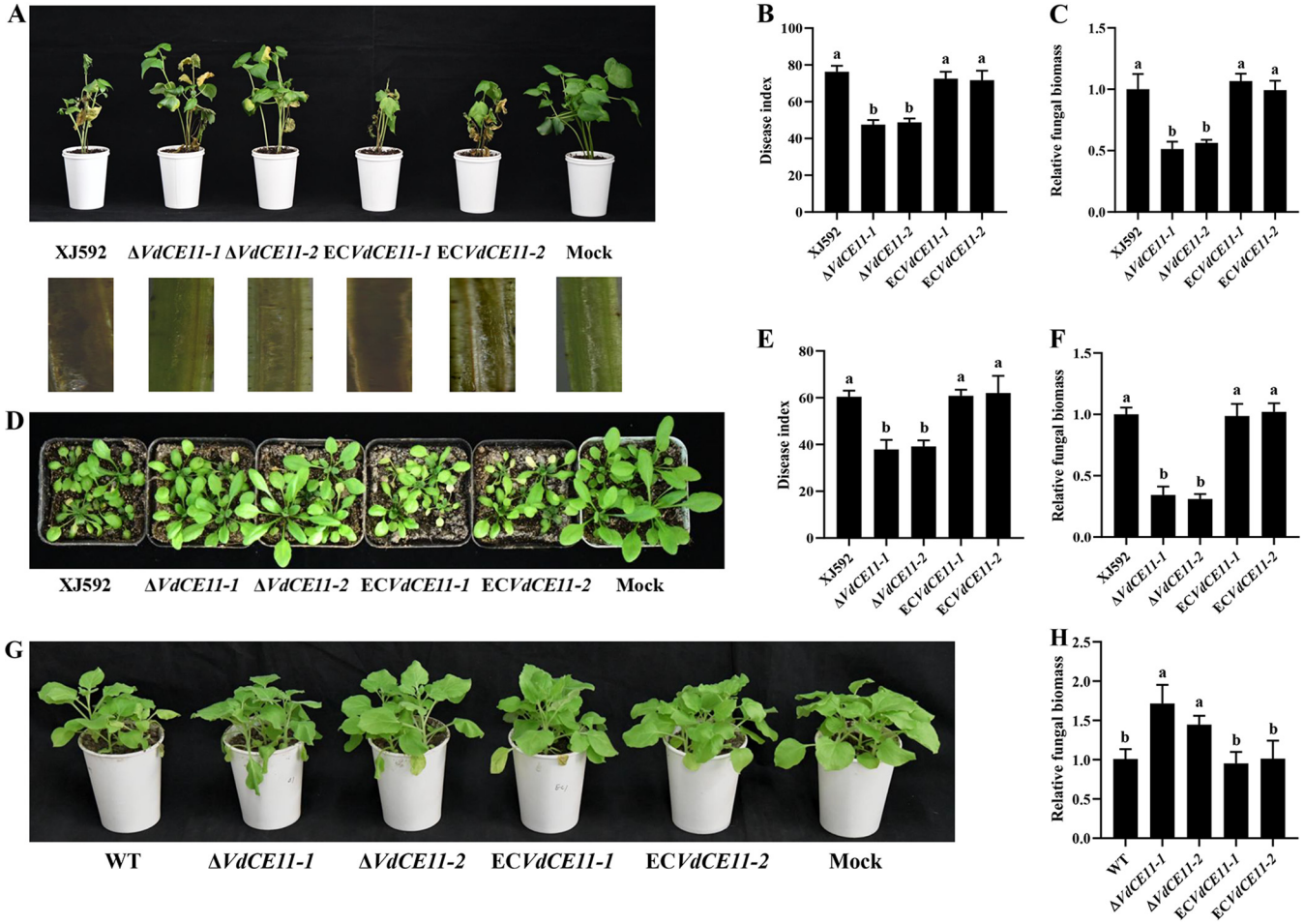

FIG 3 Detection of the pathogenesis functional diversification of VdCE11 during cotton, *Arabidopsis*, and *N. benthamiana* infection. (A) Disease symptoms of cotton infected by the indicated strains of *V. dahliae* at 14 days postinoculation (dpi). The cotton cultivar Junmian 1 was inoculated with the wild-type strain XJ592 or the mutant strains Δ*VdCE11* and EC*VdCE11*. (B) Disease index of cotton plants at 14 dpi. (C) The relative fungal biomass of cotton infected with indicated strains were determined by qPCR. *VdEF-1*α (*V. dahliae* Elongation Factor-1α) was used as a target gene, and *GhSSU* (*Gossypium hirsutum* small subunit ribosomal rRNA) was used as an internal control. (D) Disease symptoms of *Arabidopsis* infected by the indicated strains of *V. dahliae* at 14 dpi. (E) Disease index of *Arabidopsis* plants at 14 dpi. (F) The relative fungal biomass of the *V. dahliae* strains in *Arabidopsis* were determined by qPCR. *VdEF1-*α was used as target gene and *AtUBC21* (Ubiquitin-Conjugating Enzyme 21) as the *Arabidopsis* internal control gene. (G) Disease symptoms of *N. benthamiana* infected by the indicated strains of *V. dahliae* at 21 dpi. (H) The relative fungal biomasses of the *V. dahliae* strains in *N. benthamiana* were determined by qPCR. *VdEF1-*α was used as the target gene and *NbEF1-*α as the *N. benthamiana* internal control gene. Different letters represent significant differences ($P < 0.05$), according to a Student *t* test. Bars indicate the SE.

VdCE11 activates plant immunity and enhances the resistance of *N. benthamiana* to *S. sclerotiorum* and *B. cinerea* and that this function is not dependent on the SP.

Pathogenic function diversification of VdCE11. To gain insight on the expression pattern of *VdCE11* in infection and colonization of cotton roots, the roots were inoculated with conidia, collected at different time points, and the roots samples subjected RT-qPCR analysis for *VdCE11* expression. Reverse transcription-quantitative PCR (RT-qPCR) analysis indicated that expression of *VdCE11* was gradually induced during the early stage of infection (see Fig. S4A). In addition, the expression of VdCE11 was significantly induced by cotton root extract (see Fig. S4B). These results suggested that VdCE11 plays a role in plant infection.

To gain more in-depth insight into the function of VdCE11, we knocked out the *VdCE11* gene in *V. dahliae* and confirmed two mutant strains by three pairs of PCR primers (see Fig. S5A and B and Table S4). Following inoculations with the Δ*VdCE11* mutants, both cotton and *Arabidopsis* plants displayed much weaker disease symptoms than the plants inoculated with the wild-type XJ592 (Fig. 3A and D). The cotton and *Arabidopsis* plants inoculated with Δ*VdCE11* mutants also showed significantly reduced disease indices compared to those inoculated with the XJ592 strain (Fig. 3B and E). The reduced virulence of the Δ*VdCE11* mutants

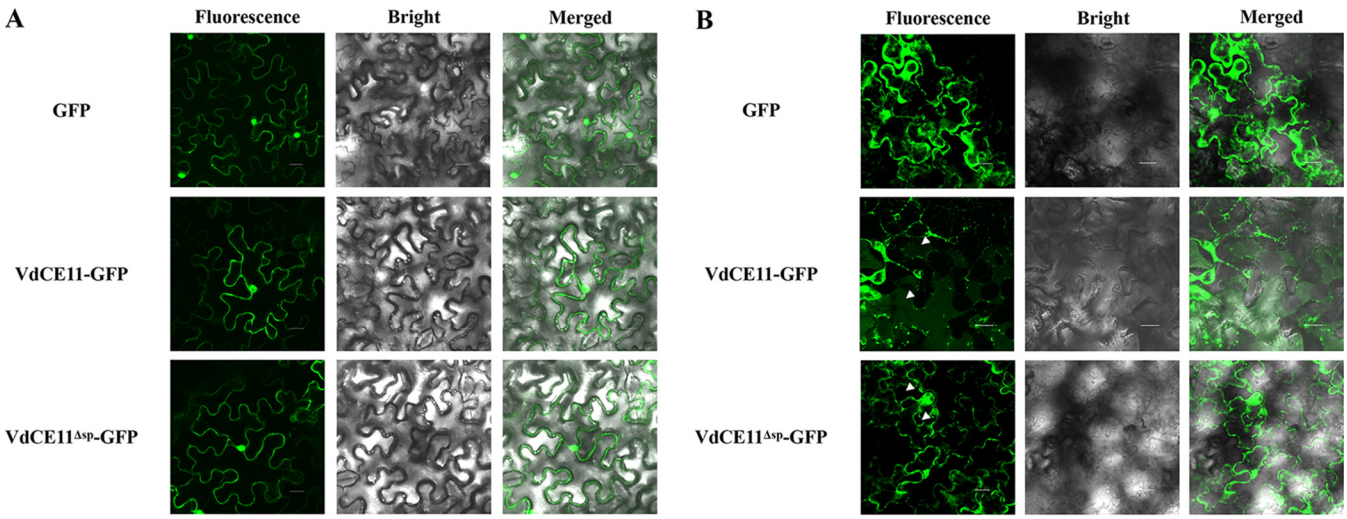

FIG 4 Subcellular localization of VdCE11 from *V. dahliae* in *N. benthamiana* epidermal cells. (A) Transient expression of GFP-tagged VdCE11 and VdCE11 without the signal peptide (VdCE11$^{\Delta sp}$) in *N. benthamiana* leaves was observed by laser scanning confocal microscopy. Pictures were taken 72 h after agroinfiltration. Scale bars, 20 μm. (B) Subcellular localization of GFP-tagged VdCE11 and VdCE11$^{\Delta sp}$ in *N. benthamiana* leaves after plasmolysis. Scale bars, 20 μm. The white arrows indicate extracellular areas.

was restored upon complementation with GFP-tagged VdCE11 (EC*VdCE11*) (Fig. 3; see also Fig. S5B). The fungal biomass and disease indices in cotton and *Arabidopsis* were consistent with the hypothesis that VdCE11 plays an important role in virulence (Fig. 3C and F). However, pathogenicity assays in *N. benthamiana* showed that deletion of *VdCE11* resulted in enhanced virulence and fungal biomass development (Fig. 3G and H). These results indicated that the virulence of *V. dahliae* in *N. benthamiana* is affected by the defense response triggered by VdCE11. There was no significant difference in growth rate or colony morphology between the Δ*VdCE11* mutants and XJ592 under normal or stressed conditions (see Fig. S5C). These results indicated that VdCE11 has a diversification function in virulence but does not affect pathogen growth.

VdCE11 localizes in the intracellular space. The localization of VdCE11 was analyzed after its expression in *N. benthamiana* leaves. While expression of VdCE11 could caused cell death in *N. benthamiana* leaves, as shown previously (Fig. 1A; see also Fig. S1), we also demonstrated that this cell death was not contingent on the presence of the SP as VdCE11$^{\Delta sp}$ could also cause cell death (see Fig. S6A). Moreover, laser scanning confocal microscopy revealed that VdCE11 was observed in both extracellular and intracellular spaces after plasmolysis (Fig. 4). However, VdCE11$^{\Delta sp}$-GFP was only observed in the intracellular space after plasmolysis (Fig. 4). Western blot analysis confirmed that both VdCE11-GFP and VdCE11$^{\Delta sp}$-GFP proteins were expressed in *N. benthamiana* leaves (see Fig. S6B). Taken together, these results indicated that VdCE11 performs its function intracellularly.

VdCE11 interacts with the aspartic protease GhAP1 of cotton. To search for the host targets of VdCE11, we performed a yeast two-hybrid (Y2H) screen with VdCE11 as the bait against a cDNA library constructed from *V. dahliae*-infected cotton roots. A cotton aspartic protease GhAP1 was identified as a candidate prey protein and the interaction between VdCE11 and GhAP1 was confirmed by Y2H (Fig. 5A; see also Fig. S7 and Table S3). Bimolecular fluorescence complementation (BiFC) assays further confirmed their interaction (Fig. 5B). Meanwhile, the luciferase signal was only captured after coexpression of VdCE11-nLUC and GhAP1-cLUC in the split-luciferase complementation imaging assay (Fig. 5C). In further support of the physical interaction between VdCE11 and GhAP1, coimmunoprecipitation assays confirmed that the GhAP1-FLAG protein coimmunoprecipitated with VdCE11-GFP when expressed in *N. benthamiana* (Fig. 5D). These results clearly demonstrated that VdCE11 interacts with GhAP1, *in vitro* and *in vivo*.

We determined the subcellular localization of GhAP1 by infiltration of a 35S:GhAP1-RFP (with and without the signal peptide) construct in *N. benthamiana* leaves. Red

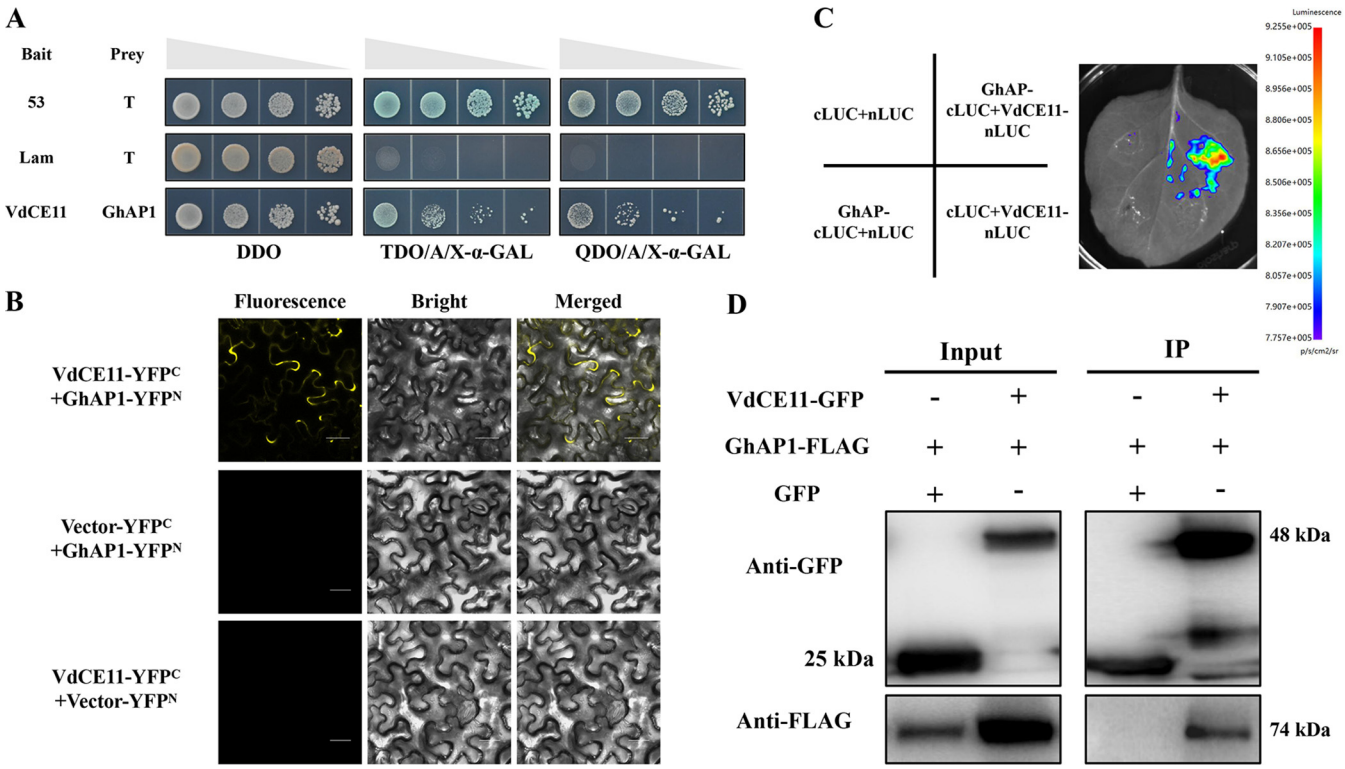

FIG 5 VdCE11 from *V. dahliae* interacts with GhAP1 from *Gossypium hirsutum* cv. Junmian 1. (A) Y2H analyses of the interaction between VdCE11 and GhAP1. Double dropout (DDO; SD/-Trp/-Leu) was used as nonselective medium, while triple dropout (TDO; SD/–Trp/–Leu/–Ade) and quadruple dropout (QDO; SD/–Trp/–Leu/–Ade/–His) as selective media. The pGBKT7-53/pGADT7-T interaction represents the positive control interaction, while pGBKT7-Lam/pGADT7-T is the negative control interaction. (B) BiFC analysis of the interaction between VdCE11 and GhAP1. VdCE11-YFP^C and GhAP1-YFP^N were transiently coexpressed in *N. benthamiana*. Scale bars, 30 μm. (C) VdCE11 interacts with GhAP1 in *N. benthamiana*. *N. benthamiana* leaves infiltrated with *Agrobacterium* strain carrying indicated constructs were subjected to split-luciferase complementation imaging assay. (D) VdCE11 interacts with GhAP1 *in planta*. VdCE11-GFP and GhAP1-FLAG were coexpressed in *N. benthamiana* leaves. Total proteins were isolated and bound by GFP-trap agarose, and the coimmunoprecipitation of VdCE11 and GhAP1 was verified by Western blotting.

fluorescence was observed in the nucleus and cytoplasm (see Fig. S8A). Coexpression of VdCE11-GFP and GhAP1-RFP (with or without the signal peptide) did not affect the localization pattern of either protein. VdCE11-GFP and GhAP1-RFP colocalized in the nucleus and cytoplasm of *N. benthamiana* cells (see Fig. S8B).

AP1 acts as a negative regulator of resistance to *V. dahliae* in cotton and *Arabidopsis*. To better understand the function of GhAP1 during the cotton-*V. dahliae* interaction, we first assayed the expression profile of GhAP1 at different times after the inoculation of cotton with *V. dahliae*. Challenge with *V. dahliae* resulted in significant induction of the transcript levels of GhAP1 at 24 h postinoculation (hpi) (see Fig. S9). Virus-induced gene silencing (VIGS) was used to specifically silence *GhAP1* gene expression (denoted as "TRV:*GhAP1*"), with TRV:00 as mock treatment and TRV:*GhCLA1* as a positive control. The cotton leaves showed an obvious photobleaching phenotype at 2 weeks after agroinfiltration with TRV:*GhCLA1* (see Fig. S10A). Meanwhile, the expression of *GhAP1* was significantly reduced in the TRV:*GhAP1* plants compared to the TRV:00 plants (see Fig. S10B). At 14 days postinoculation (dpi) with the XJ592 strain, the cotton seedlings of the TRV:*GhAP1* plants exhibited less etiolation, wilting, vascular discoloration, and leaf abscission than the TRV:00 plants (Fig. 6A). The disease index of *GhAP1*-silenced plants was significantly lower than on TRV:00 plants (Fig. 6B). Quantitative PCR (qPCR) confirmed that the fungal biomass in *GhAP1* silenced plants was also significantly lower than the mock plants (Fig. 6C). Furthermore, pathogenesis-related (*PR*) genes including *GhPR1*, *GhPR2*, *GhPR3*, *GhPR4*, *GhPR5*, *GhPR6*, and *GhPR10* were significantly upregulated in the *GhAP1*-silenced plants (Fig. 6D). These results indicate that *GhAP1* acts as a negative regulator of resistance to *V. dahliae* in cotton.

Since VdCE11 acts as an effector in *V. dahliae-Arabidopsis* interaction, we tested the interaction between AtAP1 (homolog of cotton GhAP1 in *Arabidopsis*) and VdCE11 by

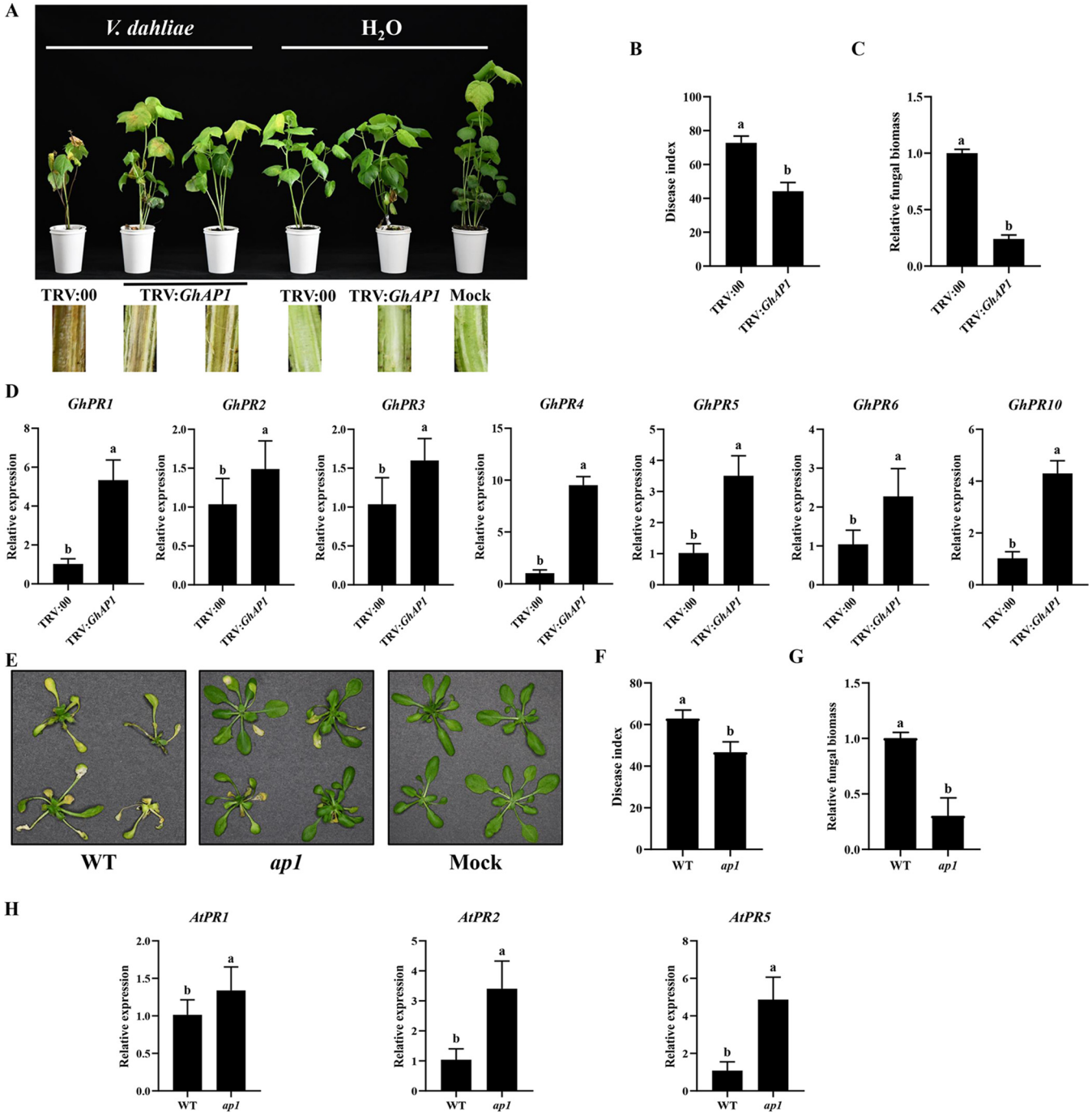

FIG 6 AP1 acts as a negative regulator of plant defense against *V. dahliae*. (A) Disease symptoms of TRV:00 and TRV:*GhAP1* plants inoculated with *V. dahliae* at 14 days postinoculation (dpi). (B) The disease index of the TRV:00 and TRV:*GhAP1* plants. (C) Biomass of *V. dahliae* in infected cotton plants determined by qPCR. *VdEF-1*α was used as a target gene and *GhSSU* as an internal control gene for qPCR. (D) Expression of *PR* genes in TRV:00 and TRV:*GhAP1* plants at 24 hpi. *GhSSU* was used as an internal control. (E) Symptoms of *V. dahliae*-infected *ap1* mutants of *A. thaliana* at 14 dpi. (F) Disease index values of WT and *ap1* plants. (G) Biomass of *V. dahliae* in infected *Arabidopsis* plants determined by qPCR. *VdEF1-*α was used as a target gene and *AtUBC21* as an internal control gene. (H) RT-qPCR analysis of the expression of *PR* genes in WT *Arabidopsis* and *ap1* plants at 24 hpi. *AtUBC21* was used as internal control. The data shown represent the means across three independent experiments. Different letters represent significant differences ($P < 0.05$), according to a Student *t* test. Bars indicate the SE.

Y2H and BiFC assays (see Table S3). The results showed that AtAP1 also interacts with VdCE11 (see Fig. S7 and Fig. S11A and B). To study whether AtAP1 plays a role in *V. dahliae* resistance, the wild-type *Arabidopsis* Col-0 and the *ap1* T-DNA insertion mutant were inoculated with strain XJ592 for the assessment of disease symptoms. As shown in Fig. 6E, the *ap1* mutant displayed higher resistance than the wild-type plants.

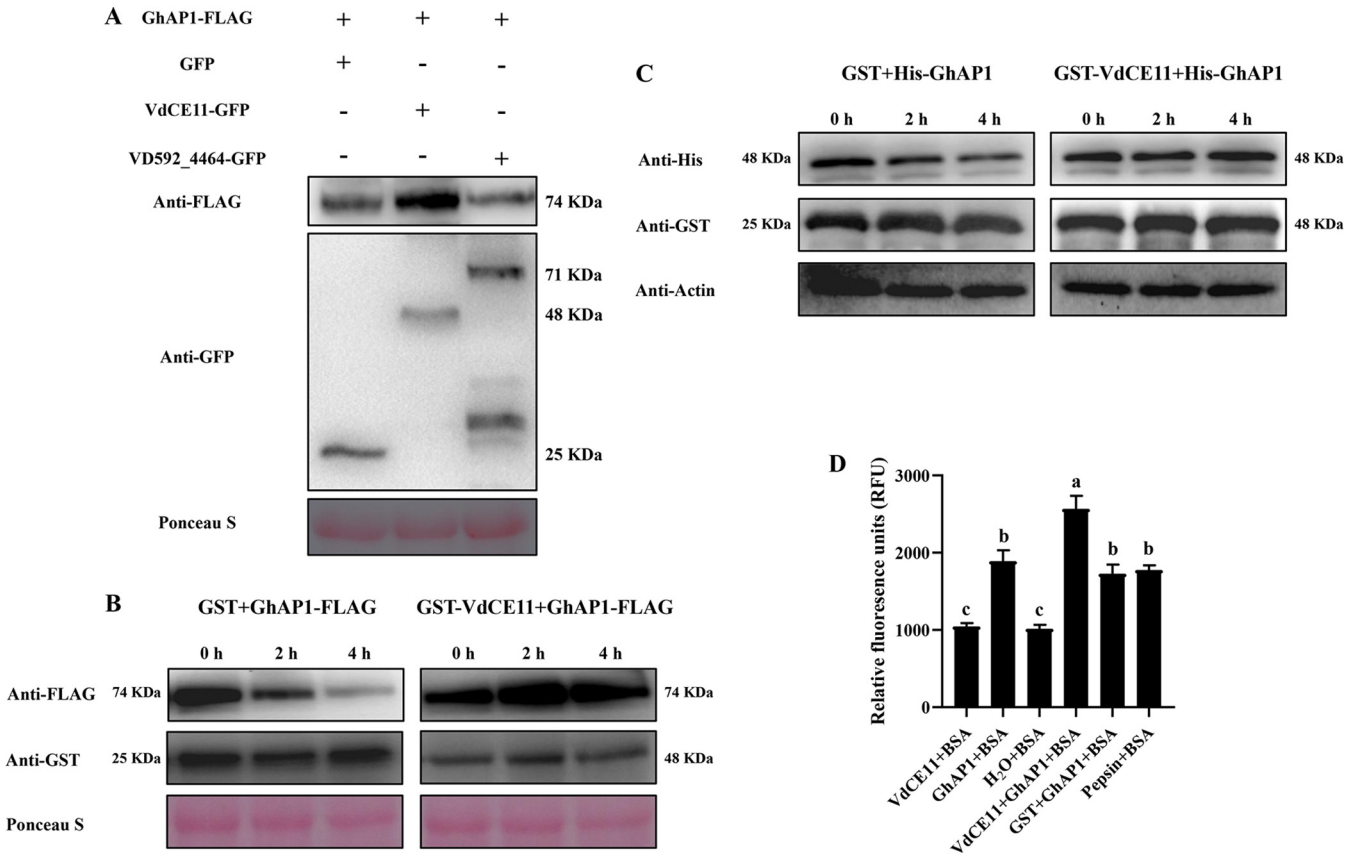

FIG 7 VdCE11 from *V. dahliae* stabilizes GhAP1 in *N. benthamiana* and activates its enzyme activity. (A) *A. tumefaciens* cells carrying the pCambia1302-VdCE11-GFP and pCambia1302-GhAP1-FLAG constructs were coinfiltrated into *N. benthamiana* leaves. VD592_4464-GFP (protein in the same family as VdCE11) and pCambia1302-GFP were used as controls. Total protein was extracted and immunoblotted with anti-GFP and anti-FLAG antibodies. Protein loading is indicated by Ponceau stain (Ponceau S). (B) *A. tumefaciens* cells carrying the pCambia1302-GhAP1-FLAG construct were infiltrated into *N. benthamiana* leaves. Total protein was extracted at 60 h after infiltration and then coincubated with the cell lysis expressed GST-VdCE11. Samples at different time points were used for Western blotting. Protein loading is indicated by Ponceau stain (Ponceau S). (C) The cell lysis expressed GST-VdCE11 and His-GhAP1 were coincubated. Samples at different time points were used for Western blot. Actin as protein loading markers. (D) Hydrolytic activity of the purified protein GST-VdCE11 and His-GhAP1 against BSA was detected. Pepsin was used as a positive control and water as a negative control. The data shown represent the means across three independent experiments. Different letters represent significant differences ($P < 0.05$), according to a Student *t* test. Bars indicate the SE.

Accordingly, the disease index and fungal biomass of *ap1* mutant plants was much lower than those of the wild-type plants at 14 dpi (Fig. 6F and G). Meanwhile, *PR* genes including *AtPR1*, *AtPR2*, and *AtPR5* were significantly upregulated in the *ap1* plants (Fig. 6H). These results indicated that the *Arabidopsis AtAP1* plays a role similar to its ortholog *GhAP1* in negatively regulating the resistance to *V. dahliae*.

VdCE11 promotes the accumulation and enzyme activity of GhAP1. To study the mechanism of interaction between VdCE11 and GhAP1, VdCE11-GFP was coexpressed with GhAP1-FLAG protein in *N. benthamiana* leaves. At 48 h postinfiltration, accumulation of GhAP1-FLAG was increased when coexpressed with VdCE11-GFP but the same accumulation of GhAP1-FLAG was not observed when it was coexpressed with the GFP control. However, the level of GhAP1-FLAG was similar when coexpressed with another Hce2 domain-containing protein (VD592_4464-GFP) which is secreted (Fig. 7A; see also Fig. S3A). VdCE11 protein also effectively inhibited the degradation of GhAP1 *in vitro*. When the cell lysis expressed glutathione *S*-transferase (GST) were coincubated with His-GhAP1 or GhAP1-FLAG, His-GhAP1 or GhAP1-FLAG proteins showed obvious degradation at 4 h of coincubation. However, it was not showed obvious degradation that the cell lysis expressed GST-VdCE11 were coincubated with His-GhAP1 or GhAP1-FLAG at 4 h (Fig. 7B and C). These results suggested that VdCE11 has a unique function in promoting the accumulation of GhAP1 *in planta*.

Since GhAP1 was annotated as a hydrolytic enzyme but lacked experimental evidence

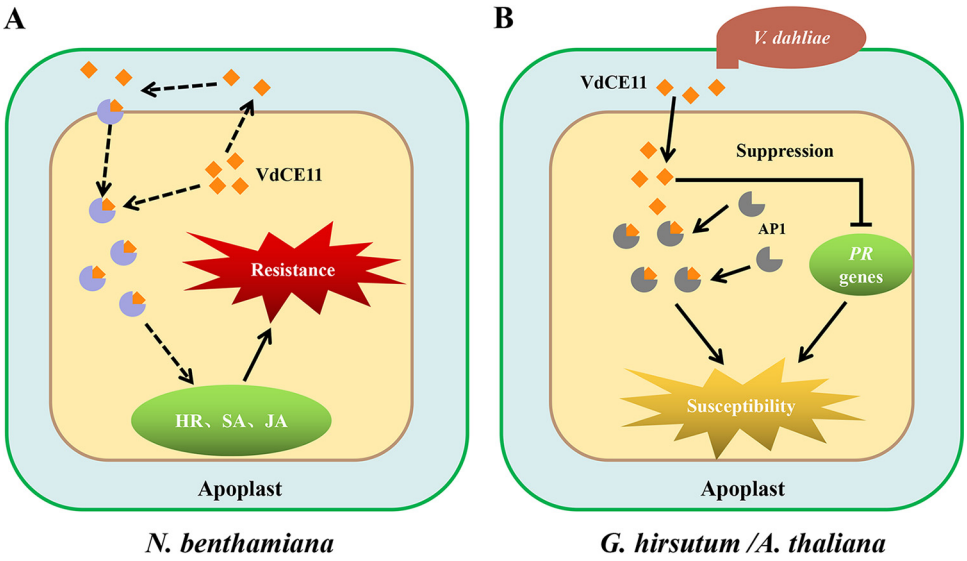

FIG 8 Model showing the predicted functional mechanism of VdCE11 in *N. benthamiana*, *G. hirsutum*, and *A. thaliana* during host-pathogen interactions. (A) In *N. benthamiana* leaves, VdCE11 may be recognized by a receptor on the cell membranes, thus stimulating the downstream HR, SA, and JA signaling pathways and promoting disease resistance of the host. (B) However, when the secreted effector VdCE11 enters cotton and *Arabidopsis* host cells, it recruits and promotes the accumulation of AP1 to make the host more susceptible to disease.

to support its activity, we tested the enzyme activity of GhAP1, revealing that it has similar activity as pepsin in hydrolyzing the bovine serum albumin (BSA) (Fig. 7D). VdCE11 increased the hydrolytic capacity of GhAP1. These results indicated that VdCE11 could enhance the hydrolytic capacity of GhAP1.

DISCUSSION

To modulate host physiology or suppress plant defense, pathogens deliver hundreds of effectors through specialized intracellular structures, such as haustoria or infection hyphae, directly into plant cells or the host apoplastic space (12). *Verticillium dahliae* secretes numerous proteins that aid in infection and collude with plant defense responses to destroy the conductivity of xylem vessels resulting in wilt symptoms (3). In this study, we identified the *V. dahliae* effector VdCE11 that induces cell death in *N. benthamiana* leaves (Fig. 1A). The yeast signal trap assay system and the subcellular localization assays revealed that VdCE11 was secreted from *V. dahliae* (see Fig. S2) and delivered into host cells. Transient expression of VdCE11 lacking the signal peptide, VdCE11$^{\Delta sp}$, also induced cell death in *N. benthamiana* (see Fig. S6A), suggesting that VdCE11 can function inside *N. benthamiana* leaves cells. Transient expression of VdCE11 in *N. benthamiana* leaf cells led to the accumulation of hydrogen peroxide and increased expression of marker genes of the HR, SA, and JA signaling pathways (Fig. 1C and D). Cotton or *Arabidopsis* infected by the Δ*VdCE11* mutants showed significantly reduced symptoms, but significantly enhanced symptoms in *N. benthamiana*, indicating that VdCE11 has a diversification function in virulence (Fig. 3). The molecular mechanism underlying VdCE11's functions may be different depending on the host, as in *N. benthamiana*, cotton, and *Arabidopsis* (Fig. 8). The literature indicates similar findings in the analyses of some other secreted proteins from *V. dahliae*. The *V. dahliae* VdEG1 and VdEG3 proteins do not induce a cotton immune response, but function as virulence factors to promote pathogen infection. However, in *N. benthamiana* leaves, VdEG1 and VdEG3 can serve as typical PAMPs whose activation depends on BAK1-mediated immune response (35). Similarly, *V. dahliae* secreted protein Vd424Y targets the nucleus of plant cells to modulate plant immunity and promote virulence but also causes cell death in *N. benthamiana* leaves (36).

Hce2, an ancient and conserved domain in the fungal kingdom, plays a central role in several effector proteins in a diverse set of hosts, and its name was derived from

homologs of *Cladosporium fulvum* Ecp2 effector protein (19). The intrinsic function of Hce2 domain-containing proteins remains unknown, but for plant-pathogenic fungi *C. fulvum* and *Mycosphaerella fijiensis*, they may function as effectors either to promote virulence or induce *R*-gene-mediated resistance in susceptible or resistant hosts, respectively (17, 37), and these functions may be conserved (19). Five Hce2 domain-containing effectors were identified in *Valsa mali*, and VmHEP1 was identified as a cell death inducer through its transient expression in *N. benthamiana*. The deletion of each single VmHEP gene did not lead to a reduction in virulence, but the double-deletion of VmHEP1 and VmHEP2 notably attenuated *V. mali* virulence in both apple leaves and twigs (38). In this study, five Hce2 domain-containing proteins were also identified in *V. dahliae* (see Fig. S3A and B). Among these, only VdCE11 could cause cell death in *N. benthamiana* leaves (see Fig. S3C). VdCE11 has an important contribution to the virulence when cotton and *Arabidopsis* were infected by *V. dahliae*, but the role is reversed in *N. benthamiana* (Fig. 3). These results provided the first evidence of the functions of Hce2 domain-containing proteins in *V. dahliae*.

The effectors secreted by plant pathogens regulate host immunity and promote pathogen infection and colonization through myriad host targets. The *Phytophthora sojae* effector Avh241 targets non-race-specific disease resistance 1 (NDR1)-like proteins, critical components of plant ETI responses and thereby inhibits ETI responses (39). The *Valsa mali* effector VmEP1 suppresses host immune responses by targeting MdPR10-mediated resistance (40). These results suggest that effectors may inhibit host basal immune responses or otherwise target the products of disease resistance genes to promote successful infection. Effectors may regulate host gene expression or protein stability to manipulate plant immunity. For example, PvRXLR111 suppresses host immunity by stabilizing VvWRKY40, which functions as a negative regulator in plant immunity (41). Two nucleus-localized effectors of the rice blast fungus modulate host immunity via transcriptional reprogramming (42). Effectors can also regulate immunity by interfering with the subcellular localization of plant proteins, regulating host physiological and biochemical reactions or regulating kinase activities (43–47). The diversity of strategies that have evolved to manipulate plant immunity via effectors likely explains the widespread occurrence of plant diseases.

Screening of a yeast two hybrid library and coimmunoprecipitation in this study revealed aspartic protease 1 (AP1) orthologs from *Arabidopsis* and cotton interact with VdCE11. Aspartic proteases, which are widely distributed in various tissues and organs of plants and animals, are involved in protein processing or degradation, senescence, stress response, programmed cell death, and reproduction (48, 49). Some studies revealed the involvement of aspartic protease in plant immunity. Prasad et al. (50) found that the heterologous expression of the aspartic protease *OsCDR1* from rice in *Arabidopsis* increased resistance to *Pseudomonas syringae* and oomyces. However, the transgenic *Arabidopsis* became more sensitive to fungus *Alternaria brassicola*, while transgenic rice showed increased resistance to *Xanomonas* and *Magnaporthe oryzae*. The enhanced disease resistance observed in transgenic plants was correlated with the expression induction of pathogenesis-related genes and enhancement of enzyme activity. Guo et al. (51) found that *VqAP13* overexpressed *Arabidopsis* showed some resistance to powdery mildew and *P. syringae* but decreased resistance to *B. cinerea*. VqAP13 promotes the SA-dependent signal transduction but suppresses the JA signal transduction pathway. Guo et al. (52) found that *Phytophthora sojae* effector PsAvh240 interacted with the soybean aspartic protease GmAP1 and reduced host resistance by suppressing GmAP1 secretion. Yang et al. (53) found an aspartic protease TiAP1 interacting with *Blumeria graminis* f. sp. *tritici* chitin deacetylase (BgtCDA1). TiAP1 in wheat may inactivate the deacetylation function of BgtCDA1, exposing chitin oligomers to wheat chitin receptors, thus triggering a wheat immune response to enhance resistance. In this study, AP1 negatively regulated the resistance of cotton or *Arabidopsis* to *V. dahliae*. Thus, we propose a new model for the mechanistic action of VdCE11 and its interaction with AP1, whereby VdCE11 promotes the accumulation and activity of AP1 and increases susceptibility of plants to *V. dahliae* (Fig. 8B).

In summary, our study indicated that VdCE11 is a cytoplasmic effector which efficiently activates plant immunity. VdCE11 also contributes to virulence by promoting the accumulation

and activity of AP1 in the host. However, further studies on how AP1 regulates plant immunity are necessary to resolve its role in promoting plant susceptibility.

MATERIALS AND METHODS

Strains and plant growth conditions. The *V. dahliae* strain XJ592 (29) was cultured on potato dextrose agar at 25°C in the dark. *Escherichia coli* DH5α (Shanghai Weidi Biotechnology Co., Ltd., China) was used for plasmid construction, and *Agrobacterium tumefaciens* GV3101(pSoup-p19) (Shanghai Weidi Biotechnology Co., Ltd., China) was used for the agroinfiltration of plants. Yeast strain YTK12 (Shanghai Weidi Biotechnology Co., Ltd., China) was used for validation of secretion and was cultured in YPRAA or CMD-W medium under dark conditions at 30°C. Yeast strain Y2H (Shanghai Weidi Biotechnology Co., Ltd., China) was used for Y2H test and was cultured in different minimal synthetically defined (SD) agar base with dropout supplements medium under dark conditions at 30°C. *A. thaliana* and *N. benthamiana* were grown in a greenhouse under a 16-h light/8-h dark cycle at 22 $\pm$ 1°C. Susceptible cultivar *Gossypium hirsutum* cv. Junmian 1 was grown in a greenhouse under a 16-h light/8-h dark cycle at 25 $\pm$ 1°C.

Bioinformatics analysis. Candidate effectors were screened by bioinformatics analysis based on the features of classic effectors ($\leq$300 amino acids, the N-terminal contains a signal peptide, no transmembrane structure, at least one disulfide bond, and no GPI-anchored domain) (54, 55). The candidate effectors were also examined using EffectorP-fungi 3.0 (https://effectorp.csiro.au/). Signal peptides were predicted using the SignalP-5.0 Server (https://services.healthtech.dtu.dk/service.php?SignalP-5.0). The transmembrane domains were predicted using Phobius (https://phobius.sbc.su.se/). GPI-anchored domains were predicted using the PredGPI (http://gpcr.biocomp.unibo.it/predgpi/pred.htm). Disulfide bonds were predicted using DiANNA (https://bio.tools/dianna). Phylogenetic dendrograms were constructed using MEGA 7 with the neighbor-joining method (56).

Plasmids construction. Coding sequences of *V. dahliae* candidate effectors were amplified from a XJ592 cDNA library with gene-specific primers using PrimeSTAR DNA polymerase (TaKaRa, Japan). These fragments were cloned into the pBin-GFP vector by using a ClonExpress OneStep cloning kit (Vazyme Biotech, China). The coding sequence of *VdCE11* without the signal peptide-encoding region was also cloned into pBin-GFP. The resulting plasmids were used for transient expression of *N. benthamiana*. For subcellular localization, *VdCE11* and *GhAP1* (without signal peptide) were cloned into the plant expression vector pCambia1302-GFP and pCambia1302-RFP, respectively. For VIGS assays, a 252-bp specific fragment of *GhAP1* and a fragment of *GhCLA1* (Cloroplastos alterados1) were cloned into pTRV2, respectively.

***Agrobacterium*-mediated infiltration assays.** *Agrobacterium*-mediated infiltration assays were performed according to the methods previously described (57). For transient expression in *N. benthamiana*, the *A. tumefaciens* GV3101 strain carrying the corresponding construct was resuspended in MES buffer (10 mM $MgCl_2$, 10 mM MES, 10 μM acetosyringone [pH 5.7]) and kept in dark for ca. 2 to 3 h before infiltration. The suspended *A. tumefaciens* cells were then injected into 4-week-old *N. benthamiana* leaves at an optical density at 600 nm (OD_{600}) of 0.5 to 0.6. Cell death was examined at 3 to 7 days postinjection.

Protein extraction and Western blotting. For transient expression analysis, total protein was extracted from the leaves of 4-week-old *N. benthamiana* plants after *Agrobacterium* infiltration. The infiltrated leaves were collected after 48 h, ground in liquid nitrogen, and mixed with an equal volume of cold protein isolation buffer (1 mM EDTA [pH 8.0], 20 mM Tris-HCl [pH 7.5], 5 mM dithiothreitol, 150 mM NaCl, 0.1% sodium dodecyl sulfate [SDS], 10% glycerol, and 1$\times$ protease inhibitor cocktail [Roche, Swiss Confederation]). The mixture was centrifuged at 4°C for 10 min at 13,000 $\times$ *g*, and then the supernatant was transferred into a new tube and boiled in protein sample buffer for 5 min. Proteins were analyzed by SDS-PAGE and electroblotted onto polyvinylidene fluoride (PVDF) membranes. PVDF membranes were blocked in Tris buffered saline 0.1% Tween 20 (TBST) containing 10% (wt/vol) nonfat dry milk at room temperature for 1 h. The primary antibody was anti-GFP (1:3,000; Abmart, China) or anti-FLAG (1:3,000; Abmart) antibody. PVDF membranes were incubated with primary antibodies in TBST with 10% (wt/vol) nonfat dry milk at room temperature for 2 h with shaking and then washed three times (5 min each) with TBST. PVDF membranes were incubated with goat anti-mouse (1:10,000; Abmart) secondary antibody in TBST at room temperature for 1 h with shaking. PVDF membranes were washed three times (5 min each) with TBST, and the signal was detected by Western blotting with chemiluminescent HRP substrate (Millipore, USA) in a ChemiDoc XRS+ system (Bio-Rad, USA).

RT-qPCR analysis. Total RNA was isolated with an RNAprep Pure Plant Plus kit (Tiangen Biotech, China) and used as the template for reverse transcription with a PrimeScript RT reagent kit (TaKaRa, Japan). The RT-qPCR assays were performed using the UltraSYBR Mixture (Cwbio, China). The cotton *GhSSU* (small subunit ribosomal rRNA) gene, the *Arabidopsis AtUBC21* (Ubiquitin-Conjugating Enzyme 21) gene, and the *N. benthamiana* and *V. dahliae EF-1*α (Elongation Factor-1α) genes were used as internal controls. The setting of thermal cycler was: predenaturation at 95°C for 10 min, followed by 40 cycles of denaturing at 95°C for 15 s, annealing at 58°C for 30 s, and extension at 72°C for 30 s. A final reaction at 72°C for 10 min was applied. Melt curves were analyzed to ensure there was not nonspecific amplification. Relative transcript levels among various samples were determined using the $2^{-\Delta\Delta CT}$ method, with three independent determinations (58). The sequences of primers used in this study are listed in Table S4.

Determination of H_2O_2 Content. Fresh tissue samples of ca. 0.1 to 0.2 g were powdered in a mortar tube together with 1 mL of acetone and quartz sand. The homogenate was centrifuged at 8,000 $\times$ *g* for 10 min at 4°C. The supernatant was placed on ice prior to testing. The content of H_2O_2 was determined according to the protocol of the Micro Hydrogen Peroxide assay kit (Solarbio, China).

Yeast signal sequence trap assay. A yeast secretion system assay was performed to validate the function of the predicted signal peptide (59). The region encoding the predicted signal of VdCE11 was

cloned into the pSUC2T7M13ori (pSUC2) vector using specific primers (see Table S4), and the resulting plasmid was transformed into an invertase mutant yeast strain YTK12 (60). The positive colonies were screened on a CMD-W medium (0.67% yeast N base without amino acids, 0.075% W dropout supplement, 2% sucrose, 0.1% glucose, 2% agar), followed by incubation on YPRAA medium (1% yeast extract, 2% peptone, 2% raffinose, 2 mg/mL antimycin A) to assay invertase secretion. The empty pSUC2 and pSUC2-Avr1b^{SP} vectors were used as negative and positive controls, respectively. Moreover, the invertase enzymatic activity was verified by the reduction of 2,3,5-triphenyltetrazolium chloride (TTC; Solarbio, China) to insoluble red triphenylformazan. Briefly, the yeast strains were incubated in 5 mL of sucrose medium for 24 h at 30°C, and the pellet was collected by brief centrifugation and then incubated with 0.1% of the colorless dye TTC at 35°C for 35 min. The invertase enzymatic activity was assayed by colorimetric changes at 5 min after incubation at room temperature.

Generation of *VdCE11* deletion and complemented strains. The upstream and downstream flanking sequences of *VdCE11* were PCR amplified from strain XJ592 genomic DNA and cloned into a pGKO-HPT vector (61). The resulting construct was transformed into *Agrobacterium tumefaciens* strain EHA105 (Shanghai Weidi Biotechnology Co., Ltd., China) and used for *A. tumefaciens*-mediated transformation (ATMT) to generate the Δ*VdCE11* mutant strain (61). The genomic region of VdCE11, including 1.5 kb upstream from the start codon, was amplified and cloned into a pNat-Tef-TrpC vector (62) to generate the construct for complementation. The resulting construct was transformed into *A. tumefaciens* EHA105 and used in ATMT to generate the Δ*VdCE11/VdCE11*-GFP strain. The primers used in this study are listed in Table S4.

Pathogenicity assays. Cotton or *Arabidopsis* plants were inoculated by the root-dip method (63). A conidial suspension of 10^7 conidia/mL from the indicated strain was used as the inoculum. The disease grade was classified as follows: grade 0 (no symptoms), grade 1 (0 to 25% wilted leaves), grade 2 (25 to 50%), grade 3 (50 to 75%), or grade 4 (75 to 100%). The disease index was calculated as follows: 100 × (sum [number of plants × disease grade])/([total number of plants] × [maximal disease grade]) (64).

For analyses of disease caused by *S. sclerotiorum* and *B. cinerea*, fresh mycelial plugs 5 mm in diameter were inoculated in agroinfiltrated areas of *N. benthamiana* leaves, 24 h after agroinfiltration with *Agrobacterium* carrying the indicated vectors. Inoculated plants were put in a transparent box to retain the humidity. The lesion diameters caused by *S. sclerotiorum* were calculated at 24 hpi. The lesion diameters caused by *B. cinerea* were calculated at 72 hpi.

Quantification of fungal biomass. For fungal biomass quantification, the stems of five plants were harvested at 14 or 21 days after inoculation for genomic DNA extraction. The fungal biomass was quantified by qPCR as described by Santhanam et al. (65). Elongation factor-1α (*EF-1α*) gene was used to quantify fungal colonization, and *GhSSU*, *AtUBC21*, *NbEF-1α* genes served as endogenous plant control. Relative fungal biomass among various samples were determined using the $2^{-\Delta\Delta CT}$ method (58).

Yeast two-hybrid screen and validation. A Y2H screen system (Shanghai OE Biotech Co., Ltd., China) was used for screens to identify candidate proteins interacting with VdCE11. For validating protein interactions, prey and bait vectors containing indicated genes were cotransformed into Y2HGold chemically competent cells (Shanghai Weidi Biotechnology Co., Ltd., China). Positive yeast clones expressing the bait-prey interacting proteins were selected from SD/–Trp–Leu medium and were replated on SD/–Trp–Leu, SD/–Trp–Leu–His and SD/–Trp–Leu–His–Ade media (Coolaber, China) for more stringent tests of bait-prey interactions.

Subcellular localization and BiFC assays. Recombinant plasmids were transformed into *A. tumefaciens* GV3101 (Shanghai Weidi Biotechnology Co., Ltd., China). The resulting strains were then infiltrated in 4-week-old *N. benthamiana* leaves according to a previously described protocol (66). At 48 h after *Agrobacterium* infiltration, the GFP, RFP, or YFP fluorescence signals within the infiltrated areas were examined using a confocal laser scanning microscope (FV3000, Japan).

Luciferase complementation assay. Plant expression vector pCambia1300-cLuc and pCambia1300-nLuc containing the fusion protein was transformed into *A. tumefaciens* GV3101 (Shanghai Weidi Biotechnology) and injected into *N. benthamiana* leaves. The reaction substrate luciferin was added at 48 h after *Agrobacterium* infiltration; then, after 5 min in the dark, the fluorescent signals were recorded for 3 min using a PlantView100 plant *in vivo* imaging system (Photon Technology, China).

Coimmunoprecipitation assays. The coding sequences of VdCE11 and GhAP1 were cloned into the plant expression vectors pCambia1302-GFP and pCambia1302-FLAG, respectively. The resulting constructs pCambia1302-VdCE11-GFP and pCambia1302-GhAP1-FLAG were introduced into *Agrobacterium* strain GV3101. *Agrobacterium* cultures carrying each construct was mixed and resuspended in MES buffer (10 mM $MgCl_2$, 10 mM MES, 10 μM acetosyringone [pH 5.7]) to a final OD_{600} of 1.0 and infiltrated into *N. benthamiana* leaves. Total proteins were isolated from *N. benthamiana* leaves 2 days after infiltration, followed by incubation with GFP-trap agarose (Chromotek, USA). The eluted proteins were analyzed by immunoblotting with anti-GFP (Abmart) or anti-FLAG (Abmart) antibodies.

Enzyme activity assay. The coding region of *VdCE11* without the signal peptide was amplified and cloned into pGEX-4T-1 while the coding region of *GhAP1* without signal peptide was amplified and cloned into pET28a. GST-VdCE11 and His-GhAP1 recombinant protein were expressed in *E. coli* strain BL21(DE3) cells (Shanghai Weidi Biotechnology). Expression of GST-VdCE11 was induced by adding 0.1 mM isopropyl-β-D-thiogalactopyrandoside (IPTG; Solabio, China) for 16 h at 16°C. Expression of His-GhAP1 was induced by adding 0.1 mM IPTG for 16 h at 25°C. Cells were collected by centrifugation at 8,000 × *g* for 10 min. Cells were lysed by an ultrasonic crusher (XM-650T, China) and sterilized by using a 0.22-mm Millex-GP filter unit (Millipore, USA). The specific method of recombinant protein purification was carried out according to the GST tag (Beyotime, China) and the His tag (Beyotime, China) protein purification kits. FITC-BSA (fluorescein isothiocyanate-bovine serum albumin; Solarbio, China) was used as the substrate for enzyme activity determination, with 20 μL per reaction. For a single target protein, 20 μL of phosphate-buffered saline (PBS) and 10 μL of purified protein were added. For two target proteins, 10 μL of PBS and 10 μL of purified protein were added for each target protein. All reactions were added

to 96-well plates. After reaction at 37°C for 0.5 h, the fluorescence was determined by using a microplate reader (Thermo Fisher Scientific, USA). For these assays, the excitation spectrum was 495 nm, and emission spectrum was 525 nm. Pepsin (Solarbio, China) was used as a positive control, and water was used as a negative control.

Data availability. Sequence data from this article can be found in the GenBank data libraries under the following accession numbers VDAG07772 (XP_009650833.1), D7B24003318 (XP_028490733.1), HYQ45013034 (KAG7125636.1), VDBG01472 (XP_003009789.1), VDAG08108 (XP_009655780.1), HYQ44020109 (KAG7100757.1), D7B24003145 (XP_028490798.1), VDBG08443 (XP_003001398.1), HYQ44011551 (KAG7109567.1), VDAG05725 (XP_009653417.1), D7B24003795 (XP_028497133.1), HYQ45001382 (KAG7142310.1), VDAG08248 (XP_009655920.1), D7B24005238 (XP_028496251.1), VDBG08578 (XP_003001533.1), HYQ44_020320 (KAG7109914.1), VDAG_09483 (XP_009656739.1), and D7B24_000774 (XP_028492408.1).

SUPPLEMENTAL MATERIAL

Supplemental material is available online only.

SUPPLEMENTAL FILE 1, PDF file, 1 MB.

ACKNOWLEDGMENTS

This study was supported by the National Key Research and Development Program of China (2018YFE0112500), the Natural Science Basic Research Program of Shannxi (2021JQ-146), and the Chinese Universities Scientific Fund (2452021136).

We thank Guo Huishan from the Institute of Microbiology, Chinese Academy of Sciences, for providing pGKO-HPT and the pNat-Tef-TrpC binary vector. We thank Si-Wei Zhang from Northwest A&F University for providing pGEX-4T-1, pER8-NeYFP, and pER8-CeYFP vectors.

REFERENCES

1. Fradin EF, Thomma BP. 2006. Physiology and molecular aspects of *Verticillium* wilt diseases caused by *V. dahliae* and *V. albo-atrum*. Mol Plant Pathol 7:71–86. https://doi.org/10.1111/j.1364-3703.2006.00323.x.
2. Klosterman SJ, Atallah ZK, Vallad GE, Subbarao KV. 2009. Diversity, pathogenicity, and management of *verticillium* species. Annu Rev Phytopathol 47:39–62. https://doi.org/10.1146/annurev-phyto-080508-081748.
3. Zhang DD, Dai XF, Klosterman SJ, Subbarao KV, Chen JY. 2022. The secretome of *Verticillium dahliae* in collusion with plant defence responses modulates *Verticillium* wilt symptoms. Biol Rev Camb Philos Soc 97:1810–1822. https://doi.org/10.1111/brv.12863.
4. Wilhelm S. 1955. Longevity of the *Verticillium* wilt fungus in the laboratory and field. Phytopathology 45:180–181.
5. Schnathorst WC. 1981. Life cycle and epidemiology of *Verticillium*, p 81–111. *In* Fungal wilt diseases of plants. Academic Press, Inc, New York, NY. https://doi.org/10.1016/B978-0-12-464450-2.50009-7.
6. Vallad GE, Subbarao KV. 2008. Colonization of resistant and susceptible lettuce cultivars by a green fluorescent protein-tagged isolate of *Verticillium dahliae*. Phytopathology 98:871–885. https://doi.org/10.1094/PHYTO-98-8-0871.
7. Zhao P, Zhao YL, Jin Y, Zhang T, Guo HS. 2014. Colonization process of *Arabidopsis thaliana* roots by a green fluorescent protein-tagged isolate of *Verticillium dahliae*. Protein Cell 5:94–98. https://doi.org/10.1007/s13238-013-0009-9.
8. Zhao YL, Zhou TT, Guo HS. 2016. Hyphopodium-specific VdNoxB/VdPls1-dependent ROS-Ca^{2+} signaling is required for plant infection by *Verticillium dahliae*. PLoS Pathog 12:e1005793. https://doi.org/10.1371/journal.ppat.1005793.
9. Dhar N, Chen JY, Subbarao KV, Klosterman SJ. 2020. Hormone Signaling and its interplay with development and defense responses in *Verticillium*-plant interactions. Front Plant Sci 11:584997. https://doi.org/10.3389/fpls.2020.584997.
10. Wang JY, Cai Y, Gou JY, Mao YB, Xu YH, Jiang WH, Chen XY. 2004. VdNEP, an elicitor from *Verticillium dahliae*, induces cotton plant wilting. Appl Environ Microbiol 70:4989–4995. https://doi.org/10.1128/AEM.70.8.4989-4995.2004.
11. Pantelides IS, Tjamos SE, Paplomatas EJ. 2010. Ethylene perception via ETR1 is required in *Arabidopsis* infection by *Verticillium dahliae*. Mol Plant Pathol 11:191–202. https://doi.org/10.1111/j.1364-3703.2009.00592.x.
12. Lo Presti L, Lanver D, Schweizer G, Tanaka S, Liang L, Tollot M, Zuccaro A, Reissmann S, Kahmann R. 2015. Fungal effectors and plant susceptibility. Annu Rev Plant Biol 66:513–545. https://doi.org/10.1146/annurev-arplant-043014-114623.
13. Chen JY, Klosterman SJ, Hu XP, Dai XF, Subbarao KV. 2021. Key insights and research prospects at the dawn of the population genomics era for *Verticillium dahliae*. Annu Rev Phytopathol 59:31–51. https://doi.org/10.1146/annurev-phyto-020620-121925.
14. Felix G, Duran JD, Volko S, Boller T. 1999. Plants have a sensitive perception system for the most conserved domain of bacterial flagellin. Plant J 18:265–276. https://doi.org/10.1046/j.1365-313X.1999.00265.x.
15. Liu T, Liu Z, Song C, Hu Y, Han Z, She J, Fan F, Wang J, Jin C, Chang J, Zhou JM, Chai J. 2012. Chitin-induced dimerization activates a plant immune receptor. Science 336:1160–1164. https://doi.org/10.1126/science.1218867.
16. Houterman PM, Cornelissen BJ, Rep M. 2008. Suppression of plant resistance gene-based immunity by a fungal effector. PLoS Pathog 4:e1000061. https://doi.org/10.1371/journal.ppat.1000061.
17. Stergiopoulos I, de Wit PJ. 2009. Fungal effector proteins. Annu Rev Phytopathol 47:233–263. https://doi.org/10.1146/annurev.phyto.112408.132637.
18. de Jonge R, van Esse HP, Kombrink A, Shinya T, Desaki Y, Bours R, van der Krol S, Shibuya N, Joosten MH, Thomma B. 2010. Conserved fungal LysM effector Ecp6 prevents chitin-triggered immunity in plants. Science 329:953–955. https://doi.org/10.1126/science.1190859.
19. Stergiopoulos I, Kourmpetis YA, Slot JC, Bakker FT, De Wit PJ, Rokas A. 2012. *In silico* characterization and molecular evolutionary analysis of a novel superfamily of fungal effector proteins. Mol Biol Evol 29:3371–3384. https://doi.org/10.1093/molbev/mss143.
20. de Jonge R, van Esse HP, Maruthachalam K, Bolton MD, Santhanam P, Saber MK, Zhao Z, Usami T, Lievens B, Subbarao KV, Thomma BPHJ. 2012. Tomato immune receptor Ve1 recognizes effector of multiple fungal pathogens uncovered by genome and RNA sequencing. Proc Natl Acad Sci U S A 109:5110–5115. https://doi.org/10.1073/pnas.1119623109.
21. Eulgem T, Somssich IE. 2007. Networks of WRKY transcription factors in defense signaling. Curr Opin Plant Biol 10:366–371. https://doi.org/10.1016/j.pbi.2007.04.020.
22. Dodds PN, Rathjen JP. 2010. Plant immunity: towards an integrated view of plant-pathogen interactions. Nat Rev Genet 11:539–548. https://doi.org/10.1038/nrg2812.
23. Tsuda K, Katagiri F. 2010. Comparing signaling mechanisms engaged in pattern-triggered and effector-triggered immunity. Curr Opin Plant Biol 13:459–465. https://doi.org/10.1016/j.pbi.2010.04.006.
24. Klosterman SJ, Subbarao KV, Kang S, Veronese P, Gold SE, Thomma BPHJ, Chen Z, Henrissat B, Lee YH, Park J, Garcia-Pedrajas MD, Barbara DJ, Anchieta A, de Jonge R, Santhanam P, Maruthachalam K, Atallah Z, Amyotte SG, Paz Z, Inderbitzin P, Hayes RJ, Heiman DI, Young S, Zeng Q, Engels R, Galagan J, Cuomo CA, Dobinson KF, Ma LJ. 2011. Comparative genomics yields insights into niche adaptation of plant vascular wilt pathogens. PLoS Pathog 7:e1002137. https://doi.org/10.1371/journal.ppat.1002137.

25. Liu T, Song T, Zhang X, Yuan H, Su L, Li W, Xu J, Liu S, Chen L, Chen T, Zhang M, Gu L, Zhang B, Dou D. 2014. Unconventionally secreted effectors of two filamentous pathogens target plant salicylate biosynthesis. Nat Commun 5:4686. https://doi.org/10.1038/ncomms5686.
26. Qin J, Wang K, Sun L, Xing H, Wang S, Li L, Chen S, Guo HS, Zhang J. 2018. The plant-specific transcription factors CBP60g and SARD1 are targeted by a *Verticillium* secretory protein VdSCP41 to modulate immunity. Elife 7: e34902. https://doi.org/10.7554/eLife.34902.
27. Gui YJ, Zhang WQ, Zhang DD, Zhou L, Short DPG, Wang J, Ma XF, Li TG, Kong ZQ, Wang BL, Wang D, Li NY, Subbarao KV, Chen JY, Dai XF. 2018. A *Verticillium dahliae* extracellular cutinase modulated plant immune responses. Mol Plant Microbe Interact 31:260–273. https://doi.org/10.1094/MPMI-06-17-0136-R.
28. Wang D, Chen JY, Song J, Li JJ, Klosterman SJ, Li R, Kong ZQ, Subbarao KV, Dai XF, Zhang DD. 2021. Cytotoxic function of xylanase VdXyn4 in the plant vascular wilt pathogen *Verticillium dahliae*. Plant Physiol 187: 409–429. https://doi.org/10.1093/plphys/kiab274.
29. Li HY, Dai JC, Qin J, Shang WJ, Chen JY, Zhang L, Dai XF, Klosterman SJ, Xu XM, Subbarao KV, Fan SH, Hu X. 2020. Genome sequences of *Verticillium dahliae* defoliating strain XJ592 and nondefoliating strain XJ511. Mol Plant Microbe Interact 33:565–568. https://doi.org/10.1094/MPMI-11-19-0320-A.
30. Pontier D, Godiard L, Marco Y, Roby D. 1994. *hsr203J*, a tobacco gene whose activation is rapid, highly localized and specific for incompatible plant/pathogen interactions. Plant J 5:507–521. https://doi.org/10.1046/j.1365-313X.1994.5040507.x.
31. Takahashi Y, Berberich T, Yamashita K, Uehara Y, Miyazaki A, Kusano T. 2004. Identification of tobacco *H1N1* and two closely related genes as spermine-responsive genes and their differential expression during the *Tobacco mosaic* virus-induced hypersensitive response and during leaf- and flower- senescence. Plant Mol Biol 54:613–622. https://doi.org/10.1023/B:PLAN.0000038276.95539.39.
32. Dean JD, Goodwin PH, Hsiang T. 2005. Induction of glutathione *S*-transferase genes of *Nicotiana benthamiana* following infection by *Colletotrichum destructivum* and *C. orbiculare* and involvement of one in resistance. J Exp Bot 56:1525–1533. https://doi.org/10.1093/jxb/eri145.
33. Seo PJ, Kim MJ, Park J-Y, Kim S-Y, Jeon J, Lee Y-H, Kim J, Park C-M. 2010. Cold activation of a plasma membrane-tethered NAC transcription factor induces a pathogen resistance response in *Arabidopsis*. Plant J 61: 661–671. https://doi.org/10.1111/j.1365-313X.2009.04091.x.
34. Asai S, Yoshioka H. 2009. Nitric oxide as a partner of reactive oxygen species participates in disease resistance to necrotrophic pathogen *Botrytis cinerea* in *Nicotiana benthamiana*. Mol Plant Microbe Interact 22:619–629. https://doi.org/10.1094/MPMI-22-6-0619.
35. Gui YJ, Chen JY, Zhang DD, Li NY, Li TG, Zhang WQ, Wang XY, Short DPG, Li L, Guo W, Kong ZQ, Bao YM, Subbarao KV, Dai XF. 2017. *Verticillium dahliae* manipulates plant immunity by glycoside hydrolase 12 proteins in conjunction with carbohydrate-binding module 1. Environ Microbiol 19: 1914–1932. https://doi.org/10.1111/1462-2920.13695.
36. Liu L, Wang Z, Li J, Wang Y, Yuan J, Zhan J, Wang P, Lin Y, Li F, Ge X. 2021. *Verticillium dahliae* secreted protein Vd424Y is required for full virulence, targets the nucleus of plant cells, and induces cell death. Mol Plant Pathol 22:1109–1120. https://doi.org/10.1111/mpp.13100.
37. Laugé R, Joosten MHAJ, Ackerveken DV, Broek HWJV, De Wit PJGM. 1997. The *in planta*-produced extracellular proteins ECP1 and ECP2 of *C. fulvum* are virulence factors. Mol Plant Microbe Interact 10:725–734. https://doi.org/10.1094/MPMI.1997.10.6.725.
38. Zhang M, Xie SC, Zhao YH, Meng X, Song LL, Feng H, Huang LL. 2019. Hce2 domain-containing effectors contribute to the full virulence of Valsa mali in a redundant manner. Mol Plant Pathol 20:843–856. https://doi.org/10.1111/mpp.12796.
39. Yang B, Yang S, Guo BD, Wang YY, Zheng WY, Tian MJ, Dai KX, Liu ZH, Wang HN, Ma ZC, Wang Y, Ye WW, Dong SM, Wang YC. 2021. The *Phytophthora* effector Avh241 interacts with host NDR1-like proteins to manipulate plant immunity. J Integr Plant Biol 63:1382–1396. https://doi.org/10.1111/jipb.13082.
40. Wang WD, Nie JJ, Lv LQ, Gong W, Wang SL, Yang MM, Xu LS, Li MJ, Du HX, Huang LL. 2021. A *Valsa mali* effector protein 1 targets apple (*Malus domestica*) pathogenesis-related 10 protein to promote virulence. Front Plant Sci 12:741342. https://doi.org/10.3389/fpls.2021.741342.
41. Ma T, Chen SY, Liu JQ, Fu PN, Wu W, Song SR, Gao Y, Ye WX, Lu J. 2021. *Plasmopara viticola* effector PvRXLR111 stabilizes VvWRKY40 to promote virulence. Mol Plant Pathol 22:231–242. https://doi.org/10.1111/mpp.13020.
42. Kim S, Kim CY, Park SY, Kim KT, Jeon J, Chung H, Choi G, Kwon S, Choi J, Jeon J, Jeon JS, Khang CH, Kang S, Lee YH. 2020. Two nuclear effectors of the rice blast fungus modulate host immunity via transcriptional reprogramming. Nat Commun 11:5845. https://doi.org/10.1038/s41467-020-19624-w.
43. McLellan H, Boevink PC, Armstrong MR, Pritchard L, Gomez S, Morales J, Whisson SC, Beynon JL, Birch PR. 2013. An RxLR effector from *Phytophthora infestans* prevents re-localization of two plant NAC transcription factors from the endoplasmic reticulum to the nucleus. PLoS Pathog 9: e1003670. https://doi.org/10.1371/journal.ppat.1003670.
44. Qi T, Guo J, Liu P, He F, Wan C, Islam MA, Tyler BM, Kang Z, Guo J. 2019. Stripe rust effector PstGSRE1 disrupts nuclear localization of ROS-promoting transcription factor TaLOL2 to defeat ROS-induced defense in wheat. Mol Plant 12:1624–1638. https://doi.org/10.1016/j.molp.2019.09.010.
45. Zhang Y, Gao YH, Wang HL, Kan CC, Li Z, Yang XF, Yin WL, Xia XL, Nam HG, Li ZH, Guo HW. 2021. *Verticillium dahliae* secretory effector PevD1 induces leaf senescence by promoting ORE1-mediated ethylene biosynthesis. Mol Plant 14:1901–1917. https://doi.org/10.1016/j.molp.2021.07.014.
46. Sabbadin F, Urresti S, Henrissat B, Avrova AO, Welsh LRJ, Lindley PJ, Csukai M, Squires JN, Walton PH, Davies GJ, Bruce NC, Whisson SC, McQueen-Mason SJ. 2021. Secreted pectin monooxygenases drive plant infection by pathogenic oomycetes. Science 373:774–779. https://doi.org/10.1126/science.abj1342.
47. Rufián JS, Rueda-Blanco J, López-Márquez D, Macho AP, Beuzón CR, Ruiz-Albert J. 2021. The bacterial effector HopZ1a acetylates MKK7 to suppress plant immunity. New Phytol 231:1138–1156. https://doi.org/10.1111/nph.17442.
48. Simões I, Faro C. 2004. Structure and function of plant aspartic proteinases. Eur J Biochem 271:2067–2075. https://doi.org/10.1111/j.1432-1033.2004.04136.x.
49. Yang Y, Feng D. 2020. Genome-wide identification of the aspartic protease gene family and their response under powdery mildew stress in wheat. Mol Biol Rep 47:8949–8961. https://doi.org/10.1007/s11033-020-05948-9.
50. Prasad BD, Creissen G, Lamb C, Chattoo BB. 2009. Overexpression of rice (*Oryza sativa* L.) OsCDR1 leads to constitutive activation of defense responses in rice and *Arabidopsis*. Mol Plant Microbe Interact 22:1635–1644. https://doi.org/10.1094/MPMI-22-12-1635.
51. Guo R, Tu M, Wang X, Zhao J, Wan R, Li Z, Wang Y, Wang X. 2016. Ectopic expression of a grape aspartic protease gene, *AP13*, in *Arabidopsis thaliana* improves resistance to powdery mildew but increases susceptibility to *Botrytis cinerea*. Plant Sci 248:17–27. https://doi.org/10.1016/j.plantsci.2016.04.006.
52. Guo BD, Wang HN, Yang B, Jiang WJ, Jing MF, Li HY, Xia YQ, Xu YP, Hu QL, Wang FF, Yu F, Wang Y, Ye WW, Dong SM, Xing WM, Wang YC. 2019. *Phytophthora sojae* effector PsAvh240 inhibits host aspartic protease secretion to promote infection. Mol Plant 12:552–564. https://doi.org/10.1016/j.molp.2019.01.017.
53. Yang Y, Fan P, Liu J, Xie W, Liu N, Niu Z, Li Q, Song J, Tian Q, Bao Y, Wang H, Feng D. 2022. *Thinopyrum intermedium* TiAP1 interacts with a chitin deacetylase from *Blumeria graminis* f. sp. *tritici* and increases the resistance to *Bgt* in wheat. Plant Biotechnol J 20:454–467. https://doi.org/10.1111/pbi.13728.
54. Choi J, Park J, Kim D, Jung K, Kang S, Lee YH. 2010. Fungal secretome database: integrated platform for annotation of fungal secretomes. BMC Genomics 11:105. https://doi.org/10.1186/1471-2164-11-105.
55. Franceschetti M, Maqbool A, Jiménez-Dalmaroni MJ, Pennington HG, Kamoun S, Banfield MJ. 2017. Effectors of filamentous plant pathogens: commonalities amid diversity. Microbiol Mol Biol Rev 81:e00066-16. https://doi.org/10.1128/MMBR.00066-16.
56. Kumar S, Stecher G, Tamura K. 2016. MEGA7: molecular evolutionary genetics analysis version 7.0 for bigger datasets. Mol Biol Evol 33:1870–1874. https://doi.org/10.1093/molbev/msw054.
57. Bos JI, Kanneganti TD, Young C, Cakir C, Huitema E, Win J, Armstrong MR, Birch PR, Kamoun S. 2006. The C-terminal half of *Phytophthora infestans* RXLR effector AVR3a is sufficient to trigger R3a-mediated hypersensitivity and suppress INF1-induced cell death in *Nicotiana benthamiana*. Plant J 48:165–176. https://doi.org/10.1111/j.1365-313X.2006.02866.x.
58. Livak KJ, Schmittgen TD. 2001. Analysis of relative gene expression data using real-time quantitative PCR and the $2^{-\Delta\Delta CT}$ method. Methods 25: 402–408. https://doi.org/10.1006/meth.2001.1262.
59. Yin W, Wang Y, Chen T, Lin Y, Luo C. 2018. Functional evaluation of the signal peptides of secreted proteins. Bio Protoc 8:e2839. https://doi.org/10.21769/BioProtoc.2839.
60. Oh SK, Young C, Lee M, Oliva R, Bozkurt TO, Cano LM, Win J, Bos JI, Liu HY, van Damme M, Morgan W, Choi D, Van der Vossen EA, Vleeshouwers VG, Kamoun S. 2009. *In planta* expression screens of *Phytophthora infestans* RXLR effectors reveal diverse phenotypes, including activation of the

Solanum bulbocastanum disease resistance protein Rpi-blb2. Plant Cell 21:2928–2947. https://doi.org/10.1105/tpc.109.068247.
61. Wang S, Xing H, Hua C, Guo HS, Zhang J. 2016. An improved single-step cloning strategy simplifies the *Agrobacterium tumefaciens*-mediated transformation (ATMT)-based gene-disruption method for *Verticillium dahliae*. Phytopathology 106:645–652. https://doi.org/10.1094/PHYTO-10-15-0280-R.
62. Zhou TT, Zhao YL, Guo HS. 2017. Secretory proteins are delivered to the septin-organized penetration interface during root infection by *Verticillium dahliae*. PLoS Pathog 13:e1006275. https://doi.org/10.1371/journal.ppat.1006275.
63. Gao F, Zhou BJ, Li GY, Jia PS, Li H, Zhao YL, Zhao P, Xia GX, Guo HS. 2010. A glutamic acid-rich protein identified in *Verticillium dahliae* from an insertional mutagenesis affects microsclerotial formation and pathogenicity. PLoS One 5:e15319. https://doi.org/10.1371/journal.pone.0015319.
64. Xu L, Zhang W, He X, Liu M, Zhang K, Shaban M, Sun L, Zhu J, Luo Y, Yuan D, Zhang X, Zhu L. 2014. Functional characterization of cotton genes responsive to *Verticillium dahliae* through bioinformatics and reverse genetics strategies. J Exp Bot 65:6679–6692. https://doi.org/10.1093/jxb/eru393.
65. Santhanam P, van Esse HP, Albert I, Faino L, Nürnberger T, Thomma BP. 2013. Evidence for functional diversification within a fungal NEP1-like protein family. Mol Plant Microbe Interact 26:278–286. https://doi.org/10.1094/MPMI-09-12-0222-R.
66. Qiao YL, Shi JX, Zhai Y, Hou YN, Ma WB. 2015. Phytophthora effector targets a novel component of small RNA pathway in plants to promote infection. Proc Natl Acad Sci U S A 112:5850–5855. https://doi.org/10.1073/pnas.1421475112.